Synthesis and Characterization of Vanadyl Phosphate Intercalated with Dioxane, Trioxane, and 18-Crown-6

Ludvík Beneš,* Vítězslav Zima, and Klára Melánová

Joint Laboratory of Solid State Chemistry, University of Pardubice, Studentská 84, 532 10 Pardubice, Czech Republic

Miroslava Trchová, Pavla Čapková, and Bohdan Koudelka

Faculty of Mathematics and Physics, Charles University, V Holešovičkách 2, 180 00 Praha, Czech Republic

Pavel Matějka

Department of Analytical Chemistry, Institute of Chemical Technology, Technická 5, 166 28 Praha, Czech Republic

Received February 4, 2002. Revised Manuscript Received April 3, 2002

Dioxane-, trioxane-, and 18-crown-6-intercalated $VOPO_4$ were prepared by a displacement reaction with 1-propanol-intercalated $VOPO_4$ and characterized by powder XRD, TGA, and UV−vis, IR, and Raman spectroscopies. Depending on the temperature of the preparation, the dioxane-intercalated $VOPO_4$ forms two compounds with formulas $VOPO_4{\cdot}C_4H_8O_2$ (the low-temperature compound) and $VOPO_4{\cdot}0.5C_4H_8O_2$ (the high-temperature compound). The former changes to the latter by heating to 70 °C. Thermal behavior of other intercalates is also discussed. The way the cyclic ethers are anchored to the $VOPO_4$ layers is inferred from the IR and Raman spectra. The arrangement of the dioxane molecules in the interlayer space of $VOPO_4$ is simulated using a *Cerius*^{2} software package combined with a *SUPRAMOL* program. In $VOPO_4{\cdot}C_4H_8O_2$, the dioxane molecules in chairlike conformation are anchored to the $VOPO_4$ layers via one of their oxygen atoms coordinated to the vanadium atoms, forming a bilayer in the interlayer space. For $VOPO_4{\cdot}0.5C_4H_8O_2$, a monolayer arrangement of the dioxane molecules is proposed.

Introduction

The tetragonal layer structure of $VOPO_4$ is made up of distorted VO_6 octahedra and PO_4 tetrahedra, which are linked by corner-sharing oxygen atoms (O_{host}).[1−3] Each octahedron is joined to four PO_4 tetrahedra and the layers are connected along the *c* axis by corner sharing the remaining two trans vertexes of the octahedron. One of these two vanadium−oxygen bonds is shorter, indicating the presence of a V═O bond while the other is much longer and can be ascribed to the coordination of a vanadyl oxygen atom from an adjacent $(VOPO_4)_\infty$ layer. Interlayer interactions are therefore accomplished by V═O···V bonds in anhydrous $VOPO_4$. In $VOPO_4{\cdot}2H_2O$, the sixth position in the VO_6 octahedron is complemented by the oxygen atom of one water molecule (O_{guest}), which is then in the trans position to the oxygen atom of the V═O bond. The second water molecule is located in the interlayer space and is H-bonded to the O_{host} atoms and to the water molecules of the first type. Vanadyl phosphate forms a number of intercalation compounds with molecular guests having Lewis base character.[4] Intercalations of aliphatic and aromatic amines,[5−9] carboxylic acids[10] and their derivatives,[11] amino acids,[12] metallocenes,[13,14] alcohols,[15−18] diols,[15,19,20] ketones,[21,22] aldehydes,[23] and

(1) Tietze, H. R. *Aust. J. Chem.* **1981**, *34*, 2035−2038.
(2) Tachez, M.; Theobald, F.; Bernard, J.; Hewat, A. W. *Rev. Chim. Mineral.* **1982**, *19*, 291−300.
(3) Jacobson, A. J. In *Encyclopedia of Organic Chemistry*; King, R. B., Ed.; Wiley: Chichester, 1994; Vol. 3, p 1556.
(4) Kalousová, J.; Votinský, J.; Beneš, L.; Melánová, K.; Zima, V. *Collect. Czech. Chem. Commun.* **1998**, *63*, 1−19.
(5) Beneke, K.; Lagaly, G. *Inorg. Chem.* **1983**, *22*, 1503−1507.
(6) Beneš, L.; Hyklová, R.; Kalousová, J.; Votinský, J. *Inorg. Chim. Acta* **1990**, *177*, 71−74.
(7) Nakajima, H.; Matsubayashi, G. *Chem. Lett.* **1993**, 423−426.
(8) Kinomura, N.; Toyama, T.; Kumada, N. *Solid State Ionics* **1995**, *78*, 281−286.
(9) De Stefanis, A.; Foglia, S.; Tomlinson, A. A. G. *J. Mater. Chem.* **1995**, *5*, 475−483.
(10) Beneš, L.; Votinský, J.; Kalousová, J.; Handlíř, K. *Inorg. Chim. Acta* **1990**, *176*, 255−259.
(11) Martinez-Lara, M.; Moreno-Real, L.; Jimenez-Lopez, A.; Bruque-Gamez, S.; Rodriguez-Garcia, A. *Mater. Res. Bull.* **1986**, *21*, 13−22.
(12) Zima, V.; Beneš, L.; Melánová, K. *Solid State Ionics* **1998**, *106*, 285−290.
(13) Matsubayashi, G.; Ohta, S. *Chem. Lett.* **1990**, 787−790.
(14) Okuno, S.; Matsubayashi, G. *Chem. Lett.* **1993**, 799−802.
(15) Beneš, L.; Melánová, K.; Zima, V.; Kalousová, J.; Votinský, J. *Inorg. Chem.* **1997**, *36*, 2850−2854.
(16) Beneš, L.; Zima, V.; Melánová, K. *J. Incl. Phenom.* **2001**, *40*, 131−138.
(17) Beneš, L.; Melánová, K.; Zima, V.; Trchová, M.; Uhlířová, E.; Matějka, P. *Eur. J. Inorg. Chem.* **2001**, 713−719.
(18) Beneš, L.; Zima, V.; Melánová, K. *Eur. J. Inorg. Chem.* **2001**, 1883−1887.
(19) Melánová, K.; Beneš, L.; Zima, V. *J. Inclusion Phenom.* **2000**, *36*, 301−309.

10.1021/cm021134+ CCC: $22.00
Published on Web 05/25/2002

poly(ethylene) glycols[24] were studied. Great attention was devoted to the intercalation of heterocyclic N- and S-donors. Pyridine and its derivatives,[25] imidazole,[26] pyrazole, pyrazine, and phenazine,[9] pyrrole and their derivatives,[27,28] 2,2′-dithiodipyridine,[29] and tetrathiafulvalene[30] were intercalated into vanadyl phosphate.

On the other hand, less attention has been paid to the intercalation of heterocycles with O-donor. Recently, tetrahydrofuran and tetrahydropyran have been intercalated into vanadyl phosphate.[31,32] It is presumed that the guests are coordinated to the vanadium atoms of the host layer through free electron pairs of the donor O atoms of the guests. In this paper, we report on the preparation and characterization of intercalates with cyclic ethers containing two or more oxygen heteroatoms, that is, 1,4-dioxane, 1,3,5-trioxane, and 18-crown-6.

Experimental Section

Preparation. The intercalation compounds were obtained by a displacement reaction. The solid propanol intercalate[15] was prepared in advance and used as a starting material for the reaction with the corresponding guest. The composition of the intercalates prepared was determined by elemental analyses (C, H).

$VOPO_4 \cdot C_4H_8O_2$. The propanol intercalate (1 g) was suspended in 50 mL of dioxane and stirred for 1 day at laboratory temperature. The product was separated by filtration and dried in nitrogen. Anal. Calcd. for $VOPO_4 \cdot C_4H_8O_2$: C, 19.22%; H, 3.22%. Found: C, 19.61%; H, 3.39%.

$VOPO_4 \cdot 0.5C_4H_8O_2$. The propanol intercalate (1 g) was suspended in 50 mL of dioxane and refluxed for 1 h. The product was filtered off and dried in nitrogen. Anal. Calcd. for $VOPO_4 \cdot 0.5C_4H_8O_2$: C, 11.66%; H, 1.96%. Found: C, 11.61%; H, 2.04%.

$VOPO_4 \cdot C_3H_6O_3$. The propanol intercalate (1 g) was suspended in 50 mL of the acetonitrile solution of trioxane (1 g) and refluxed for 2 h. The product was filtered off and dried in nitrogen. Anal. Calcd. for $VOPO_4 \cdot C_3H_6O_3$: C, 14.30%; H, 2.40%. Found: C, 14.15%; H, 2.33%.

$VOPO_4 \cdot 0.5C_3H_6O_3$. The trioxane intercalate ($VOPO_4 \cdot C_3H_6O_3$) was heated at 180 °C in vacuo for 15 min. Anal. Calcd. for $VOPO_4 \cdot 0.5C_3H_6O_3$: C, 8.71%; H, 1.46%. Found: C, 8.45%; H, 1.50%.

$VOPO_4 \cdot 0.43C_{12}H_{24}O_6$. The propanol intercalate (1 g) was suspended in 50 mL of the toluene solution of 18-crown-6 (2.5 g) and stirred for 1 week at room temperature. The product was filtered off and dried in nitrogen. Anal. Calcd. for $VOPO_4 \cdot 0.43C_{12}H_{24}O_6$: C, 22.49%; H, 3.78%. Found: C, 22.61%; H, 3.59%.

XRD. Powder data were obtained with an X-ray diffractometer HZG-4 (Freiberger Präzisionsmechanik, Germany) using Cu Kα radiation with discrimination of the Cu Kβ radiation by a Ni filter. Diffraction angles were measured from 5 to 50° (2θ). The temperature measurements from 20 to 250 °C were carried out on a heated corundum plate with thermocouple.[33]

Density. The density was measured with an automated helium pycnometer (AutoPycnometer 1320, Micromeritics, Norcross, GA, USA) to 0.01 g/cm^3 accuracy.

Thermogravimetry. The TG analyses were performed using a Derivatograph C (MOM Budapest, Hungary). The measurements were carried out in air between 20 and 600 °C at a heating rate of 5 K/min.

UV−Vis Spectroscopy. UV−vis diffuse reflectance spectra were measured on a dual-beam UV−vis−NIR spectrometer JASCO V570 equipped with an integrating sphere attachment ISN-470.

IR Spectra. Infrared spectra in the ranges 650−2000 and 2600−3100 cm^{-1} were obtained with a fully computerized Nicolet IMPACT 400 FTIR spectrometer (300 scans/spectrum at 2-cm^{-1} resolution). The spectra of the intercalates and the solid hosts were measured in KBr pellets in the transmission mode; the spectrum of liquid dioxane was measured by an ATR technique on a ZnSe crystal. The spectra were corrected for the H_2O and CO_2 content in the optical path.

Raman Spectra. FT Raman spectra were collected using a Fourier transform near-infrared (FT-NIR) spectrometer Equinox 55/S (Bruker) equipped with FT Raman module FRA 106/S (Bruker) (128 interferograms were co-added per spectrum in the range 4000 to −1000 cm^{-1} at 4-cm^{-1} resolution).

Molecular Simulations. The program *SUPRAMOL*[34] combined with a *Cerius*^{2} software package[35] was used in the structure analysis of the low-temperature and high-temperature phases of vanadyl phosphate intercalated with dioxane. As evident from the diffraction patterns, both phases differ in the basal spacing and arrangement of the guest molecules in the interlayer space. Because of the strong preferred orientation of crystallites, the 00*l* basal reflections are predominant in the diffraction pattern. The weak and broad *hk*0 and *hkl* reflections indicate a disorder in the layer stacking due to a disorder of the guest molecules. The effect of the disorder is stronger in the diffraction pattern of the low-temperature phase of $VOPO_4$ intercalated with dioxane. The weak resolution of the powder diffraction patterns for both phases did not allow us to solve the structure from the diffraction analysis only. In such a case the molecular simulations are very powerful tools in structure analysis.

The strategy of the modeling is based on the data from two experimental methods: X-ray powder diffraction and vibration spectroscopy. From the powder diffraction data we obtained the values of the basal spacing. The infrared spectra of the anhydrous vanadyl phosphate and its hydrated form were compared with the spectra of the low- and high-temperature phases of the intercalated structure. From this comparison we deduce that the main spectral bands corresponding to the $VOPO_4$ layer remain unchanged after the intercalation. It means that the host layers can be treated as rigid units during energy minimization.

The program *SUPRAMOL*[34] was used to generate initial models for the molecular mechanics simulations. *SUPRAMOL* creates systematically a grid of the initial models, which cover the entire space given by all degrees of freedom, that is, the positions, orientations, and subrotations of the intercalated molecules. Each node of this grid represents a single initial

(20) Beneš, L.; Melánová, K.; Zima, V. *J. Solid State Chem.* **2000**, *151*, 225−230.
(21) Melánová, K.; Beneš, L.; Zima, V.; Čapková, P.; Trchová, M. *Collect. Czech. Chem. Commun.* **1999**, *64*, 1975−1979.
(22) Čapková, P.; Trchová, M.; Zima, V.; Schenk, H. *J. Solid State Chem.* **2000**, *150*, 356−362.
(23) Melánová, K.; Beneš, L.; Zima, V.; Votinský, J. *J. Solid State Chem.* **2001**, *157*, 50−55.
(24) Melánová, K.; Beneš, L.; Zima, V.; Vahalová, R.; Kilián, M. *Chem. Mater.* **1999**, *11*, 2173−2178.
(25) Johnson, J. W.; Jacobson, A. J.; Brody, J. F.; Rich, S. M. *Inorg. Chem.* **1982**, *21*, 3820−3825.
(26) De Stefanis, A.; Tomlinson, A. A. G. *J. Mater. Chem.* **1994**, *5*, 319−322.
(27) Matsubayashi, G.; Nakajima, H. *Chem. Lett.* **1993**, 31−34.
(28) Nakajima, H.; Matsubayashi, G. *J. Mater. Chem.* **1994**, *4*, 1325−1329.
(29) Yatabe, T.; Matsubayashi, G. *J. Mater. Chem.* **1996**, *6*, 1849−1852.
(30) Pozas-Tormo, R.; Moreno-Real, L.; Bruque-Gamez, S.; Martinez-Lara, M.; Ramos-Barado, J. *Mater. Sci. Forum* **1992**, *91−93*, 511−516.
(31) Goubitz, K.; Čapková, P.; Melánová, K.; Molleman, W.; Schenk, H. *Acta Crystallogr.* **2001**, *B57*, 178−183.
(32) Zima, V.; Melánová, K.; Beneš, L.; Trchová, M.; Čapková, P.; Matějka, P. *Chem. Eur. J.* **2002**, *8*, 1703−1709.
(33) Beneš, L. *Sci. Pap. Univ. Pardubice Ser. A* **1996**, *2*, 151−155.
(34) Koudelka, B.; Čapková, P. *SUPRAMOL*—Computer Program; Faculty of Mathematics and Physics, Department of Chemical Physics and Optics, Charles University: Prague, Czech Republic, 2001.
(35) *Cerius*^{2} documentation; Molecular Simulation Inc.: San Diego, June 2000.

model of the structure. Two criteria for the final choice of the initial models are applied in *SUPRAMOL*: (1) similarity of the experimental and calculated diffraction patterns and (2) minimum of van der Waals energy, which estimates good crystal packing. Initial models fulfilling these two criteria are chosen for the more sophisticated minimization procedure in *Cerius*[2].

Energy minimization was carried out in a *Minimize*r module of *Cerius*[2] *4.5* using the *Universal force field*[36] under the following constraints: rigid but movable host layers, fixed V−O_{diox} distance, and variable positions of all atoms in the dioxane molecules, with exception of the O_{diox}. The cell parameters *a*, *b*, and γ were kept fixed and *c*, α, and β were variable during the energy minimization.

Results and Discussion

Synthesis and Characterization. None of the guests can be intercalated directly into anhydrous vanadyl phosphate and also replacement of the water molecules in $VOPO_4 \cdot 2H_2O$ does not lead to an intercalation. The intercalates had to be prepared by replacing 1-propanol molecules in the corresponding $VOPO_4$ intercalates. In the case of dioxane, two intercalates can be prepared depending on the temperature of the preparation (room temperature, denoted l.t.; reflux, denoted h.t.). The intercalates prepared are yellow crystalline solids, indicating that the vanadium(V) is not significantly reduced. As follows from the elemental analyses and TG measurements, the stoichiometry of the intercalates prepared can be expressed as $VOPO_4 \cdot$ dioxane (l.t. intercalate), $VOPO_4 \cdot 0.5$dioxane (h.t. intercalate), $VOPO_4 \cdot$trioxane, and $VOPO_4 \cdot 0.43$(18-crown-6).

Similar to the tetrahydrofuran and tetrahydropyran intercalates,[32] all the intercalates studied are more stable in air (at 40−50% relative humidity) than the 1-alkanol,[15] 1,2-alkanediol,[19] or acetone[21] intercalates. The presence of the (001) diffraction line of vanadium phosphate dihydrate was not observed in the product even after more than 7 days, whereas for acetone-intercalated $VOPO_4$ this line appears after 1 h of standing in air. Only the dioxane (l.t.) intercalate changes to the h.t. phase by standing in air.

The diffractograms of all intercalates show a series of sharp (00*l*) reflections (see Figure 1). The diffractograms of the 18-crown-6 and dioxane (l.t.) intercalates contain also (200) and (201) reflections. The lattice parameters of the tetragonal structure are $a = 6.22$ Å and $c = 13.60$ Å for the 18-crown-6 intercalate and $a = 6.20$ Å and $c = 11.56$ Å for the dioxane (l.t.) intercalate. In the case of the trioxane intercalate, the *a* parameter was determined from the (200) line and the lattice parameters are $a = 6.21$ Å and $c = 9.22$ Å. The diffractogram of the dioxane (h.t.) intercalate contains two (00*l*) reflections (with the basal spacing of 7.89 Å) and a low intensive reflection with $d = 3.04$ Å, which could correspond to the (200) line for $a = 6.08$ Å. It would mean an unusual decrease of the *a* parameter of the tetragonal host lattice. If we suppose that the *a* parameter of the host does not change during intercalation, this reflection could be a (201) line for $a = 6.20$ Å and $c = 15.78$ Å. Thus, the lattice parameters of this intercalate cannot be unequivocally determined.

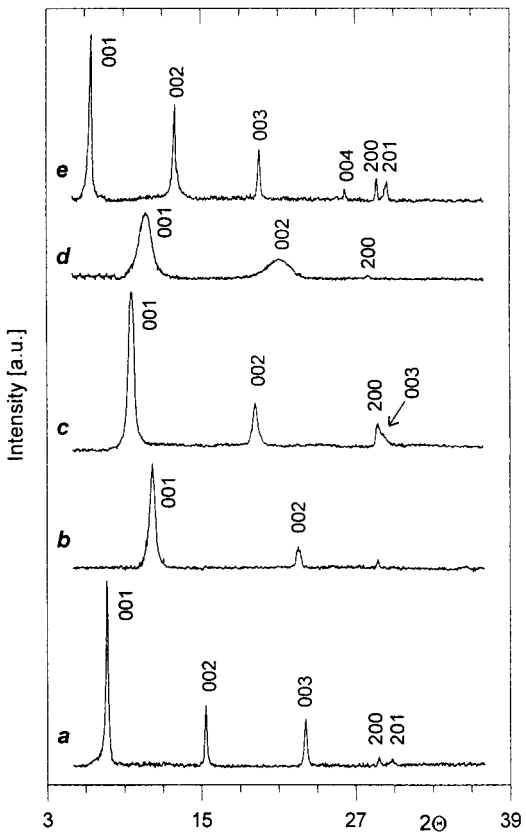

Figure 1. Diffractograms of vanadyl phosphate intercalated with dioxane (l.t.) (a), dioxane (h.t.) (b), trioxane (c), trioxane after heating at 180 °C in vacuo (d), and 18-crown-6 (e).

Thermal Behavior. The dioxane intercalate prepared at room temperature (l.t.) is not very stable at higher temperatures; it very easily releases a part of the guest and changes to a phase with the basal spacing of 7.89 Å. Both phases are present in the temperature region from 50 to 70 °C. The (00*l*) diffraction lines of both phases are distinctly broadened in this temperature range. Only one phase, which is identical to the dioxane intercalate prepared by refluxing (h.t.), is present above 70 °C. This intercalate is extremely thermally stable because the position and intensity of the diffraction lines do not change up to 270 °C. Above this temperature, the intensity of the diffraction lines decreases and dioxane is released slowly. The degree of reduction of vanadium(V) to vanadium(IV) in the freshly prepared dioxane intercalates (both l.t. and h.t. forms) and the product obtained by their heating to 260 °C was followed by visible reflectance spectroscopy and compared with the spectra of $VOPO_4 \cdot 2H_2O$ (containing only vanadium(V)) and $Na_{0.015}VOPO_4 \cdot 2H_2O$ (with 1.5% of vanadium(IV)). The spectra of the intercalates prepared are similar to that of $VOPO_4 \cdot 2H_2O$, which indicates that vanadium(V) is not significantly reduced. Even heating to 260 °C does not lead to a great reduction of vanadium(V). The high thermal stability of the h.t. form of the dioxane intercalate indicates a very strong interaction between the guest species and the host layers.

Similar thermal behavior was observed for the trioxane intercalate. The phase with the basal spacing of 9.22 Å is stable up to 145 °C. In the temperature range 145−200 °C, a phase with basal spacing of 7.90−8.17 Å exists. The diffractograms of this phase show very

(36) Rappe, A. K.; Casewit, C. J.; Colwell, K. S.; Goddard, W. A.; Skiff, W. M. *J. Am. Chem. Soc.* **1992**, *114*, 10024−10035.

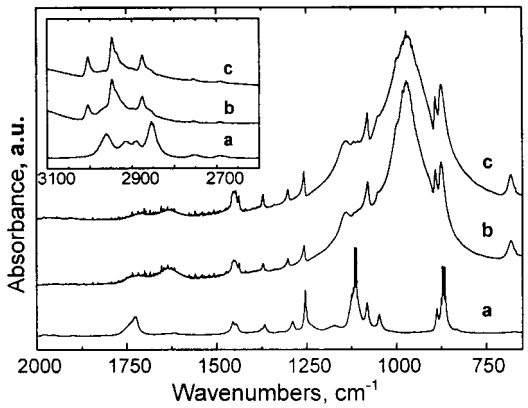

Figure 2. FTIR spectra of liquid dioxane (ATR on ZnSe crystal) (a), vanadyl phosphate intercalated with dioxane (l.t.) (in KBr pellet) (b), and vanadyl phosphate intercalated with dioxane (h.t.) (in KBr pellet) (c).

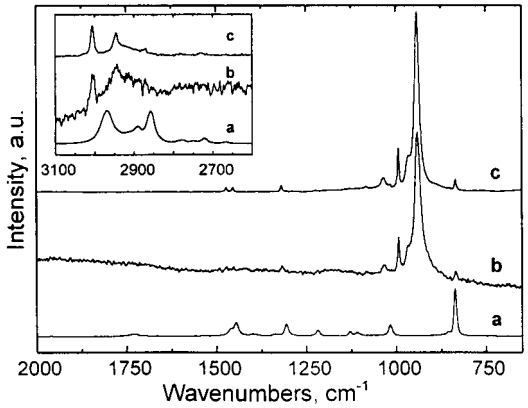

Figure 3. Raman spectra of liquid dioxane (a), vanadyl phosphate intercalated with dioxane (l.t.) (b), and vanadyl phosphate intercalated with dioxane (h.t.) (c).

broad (00*l*) lines and a (200) line (see Figure 1d), which makes it possible to determine the value of the *a* parameter (6.21 Å). Green color of this phase indicates that it contains a significant amount of vanadium(IV). We succeeded in the preparation of this phase by heating the trioxane intercalate at 180 °C in vacuo for 15 min. As follows from the thermogravimetric analysis, the high-temperature phase contains one-half of the initial amount of trioxane. The final product of the decomposition at 700 °C is anhydrous vanadyl phosphate.

As follows from the diffractograms, the 18-crown-6 intercalate is thermally stable up to 160 °C. At higher temperatures, a fast decomposition was observed.

Infrared and Raman Spectra. The infrared and Raman spectra of liquid dioxane and vanadyl phosphate intercalated with dioxane (l.t. and h.t.) are given in Figures 2 and 3. The spectra of the dioxane intercalates (l.t. and h.t.) are very similar.

The positions of the main spectral bands of the host structure—$(VOPO_4)_\infty$—in the spectrum of the intercalates only slightly differ from those of anhydrous vanadyl phosphate or its hydrated form.[37] It confirms that the structure of the original $VOPO_4$ layers remains unchanged after the intercalation reaction. The intense band at 941 cm^{-1} in the Raman spectrum corresponds to the symmetric $\nu(PO_4)$ stretching vibration in the host layers and it is observed at 968 cm^{-1} in the infrared spectrum. The position of the V=O stretching vibration at 993 cm^{-1} in the Raman spectrum (observed at 1004 and 995 cm^{-1} for the 5-hexyn-1-ol and THP intercalates, respectively)[17,32] indicates a coordination of O_{guest} to the vanadium atom of the host. This band is observed as a shoulder at about 998 cm^{-1} (1007, 1002, and 995 cm^{-1} for 5-hexyn-1-ol,[17] acetone,[21,22] and THP[32] intercalates, respectively) in the infrared spectrum, allowing us to distinguish this band from other bands belonging to the intercalated dioxane molecules. The vanadyl stretching band appears to be especially sensitive to the atoms coordinated to vanadium within an octahedral arrangement in the host lattice structure. For instance, when water molecules are intercalated into $VOPO_4$, the position of this band at 1035 cm^{-1} in anhydrous vanadyl phosphate changes to 995 cm^{-1}, typical for mono- and dihydrate.[37] High thermal stability of the dioxane (h.t.) intercalate indicates a very strong host—guest interaction that corresponds well with the observed position of the vanadyl stretching band in the dioxane intercalate. The band at 1142 cm^{-1} in the infrared spectrum of the intercalate with dioxane is an asymmetric $\nu(PO_4)$ vibration.

Dioxane has a chair conformation in vapor and in solution. The normal vibrations were classified as localized to CH_2 stretching, scissoring, wagging, twisting, and rocking and to ring stretching and bending vibrations.[38,39] A large degree of mixing, particularly between the CH_2 twisting and rocking vibrations and some of the ring stretching modes, were indicated. The infrared and Raman spectra of dioxane differ in the position, shape, and intensity of the corresponding bands in the intercalate structure as a consequence of the intercalation reaction in the interlayer space. The remarkable change of the CH_2 stretching vibrations was observed when going from liquid pure dioxane to its intercalated form. By fixation of the intercalated molecules in the interlayer space, the asymmetric CH_2 stretching vibrations at 2961, 2917, 2881, and 2854 cm^{-1} shift to 3003, 2947, 2904 (a shoulder), and 2874 cm^{-1} in the infrared spectrum (Figure 2). The shifts from 2967, 2891, and 2858 cm^{-1} to 3005, 2945, and 2871 cm^{-1} are observed in the Raman spectrum (Figure 3). In the spectrum of the dioxane (l.t.) intercalate a shoulder at 2917 cm^{-1} can be observed, corresponding to the free dioxane molecules present in the sample. It agrees with the fact that the dioxane intercalate prepared at room temperature (l.t.) is not very stable and it very easily releases a part of the guest at higher temperatures. The Raman spectrum of the dioxane (l.t.) intercalate is strongly influenced by the baseline radiation (not observed in the spectrum of the dioxane (h.t.) intercalate), which may be caused by the presence of free dioxane molecules.

By intercalation, the change of the scissoring (from the doublet at 1456 and 1444 cm^{-1} in the liquid guest to 1454 cm^{-1} in the intercalate), wagging (from 1368 to

(37) Trchová, M.; Čapková, P.; Matějka, P.; Melánová, K.; Beneš, L. *J. Solid State Chem.* **1999**, *148*, 197−204.

(38) Ellestad, O. H.; Klaboe, P.; Hagen, G. *Spectrochim. Acta* **1971**, *27A*, 1025−1048.

(39) Pickett, H. M.; Strauss, H. L. *J. Chem. Phys.* **1970**, *53*, 376−388.

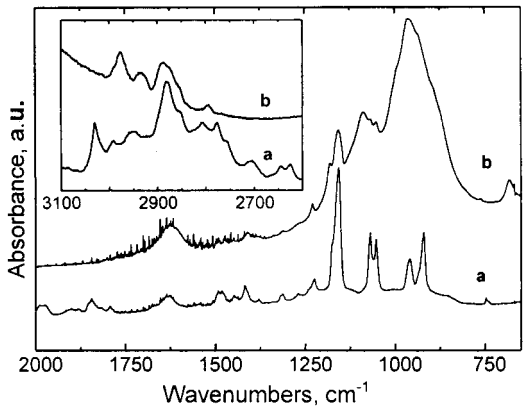

Figure 4. FTIR spectra of polycrystalline trioxane (in KBr pellet) (a) and vanadyl phosphate intercalated with trioxane (in KBr pellet) (b).

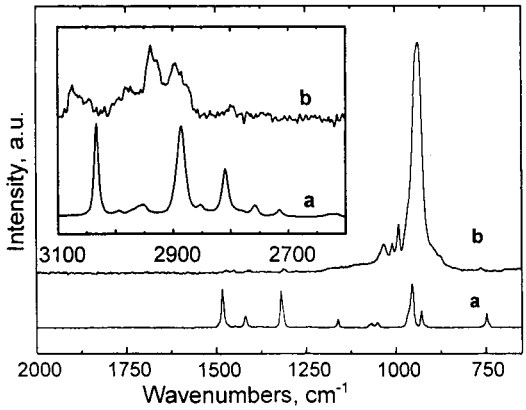

Figure 5. Raman spectra of trioxane (a) and vanadyl phosphate intercalated with trioxane (b).

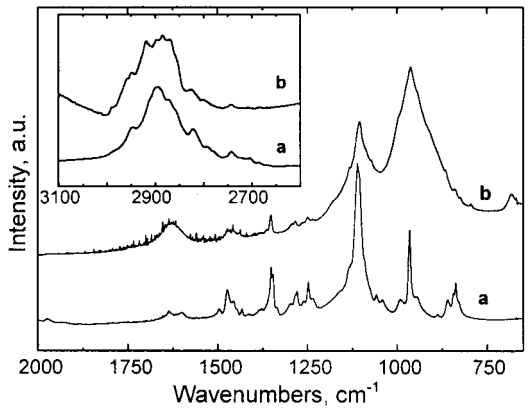

Figure 6. FTIR spectra of polycrystalline 18-crown-6 (in KBr pellet) (a) and vanadyl phosphate intercalated with 18-crown-6 (in KBr pellet) (b).

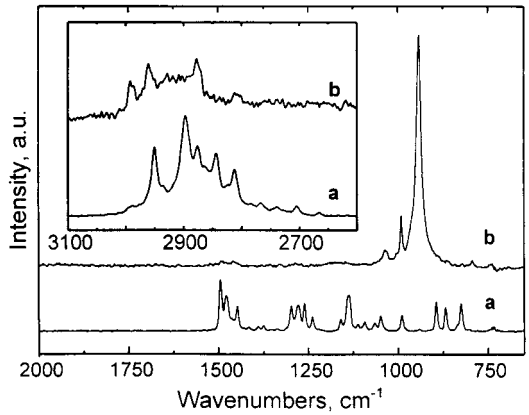

Figure 7. Raman spectra of 18-crown-6 (a) and vanadyl phosphate intercalated with 18-crown-6 (b).

1374 cm^{-1}), twisting (from 1290 and 1255 cm^{-1} to 1302 and 1261 cm^{-1}, respectively), and rocking (from 1082 and 869 cm^{-1} to 1079 and 875 cm^{-1}, respectively) vibrations of CH_2 of dioxane were observed in the infrared spectrum. The bands of the symmetric C−O−C ring vibrations at 869 cm^{-1} keep the same position in the pristine guest compound and in the high- and low-temperature phases of the intercalate. However, the antisymmetric C−O−C ring vibrations at 1290 and 1117 cm^{-1}, overlapped by the PO_4 vibrations of vanadyl phosphate, are shifted to the lower wavenumbers in the infrared spectrum of the high- and low-temperature phase of the intercalate. The observed changes are a consequence of the host−guest and guest−guest interactions in the interlayer space of $VOPO_4$.

The infrared and Raman spectra of polycrystalline trioxane and vanadyl phosphate intercalated with trioxane are given in Figures 4 and 5. The intense broad band centered at about 938 cm^{-1} in the Raman spectrum of the intercalate with trioxane corresponds most probably to the symmetric $\nu(PO_4)$ vibration[37] overlapped by the strong band of trioxane. The sharp band at 992 cm^{-1} corresponds to the V═O stretching vibration. Interpretation of this region in the infrared spectrum is rather complicated. The $\nu(PO_4)$ stretching vibration, the V═O stretching vibration, and the C−O−C stretching vibration of the guest overlap in this part of the spectrum. With the help of the Raman spectrum, the band at 961 cm^{-1} in the infrared spectrum was assigned to the symmetric $\nu(PO_4)$, which is infrared active because of the distortion of the phosphate tetrahedron in the intercalate. The shoulder at about 993 cm^{-1} is most probably the V═O stretching band corresponding to the anchoring of the oxygen of trioxane to the vanadium atom. The band at about 1089 cm^{-1} may be an asymmetric $\nu(PO_4)$ vibration, which is observed at 1033 cm^{-1} in the Raman spectrum.

Only some of the bands of polycrystalline trioxane (Figures 4 and 5) are observed in the spectra of the intercalate. In the infrared spectrum of the intercalate, we observed an antisymmetric ring vibration at about 1157 cm^{-1} with a shoulder at 1181 cm^{-1}. A doublet of antisymmetric ring vibrations at about 1069 and 1054 cm^{-1} is at the same position in the infrared spectrum after the intercalation. The band of the twisting vibration of CH_2 at 1224 cm^{-1} is shifted to 1156 cm^{-1} in the intercalate. The band at about 1621 cm^{-1} corresponds to the bending vibration of the water molecules in the KBr pellet. During the fixation of the intercalated molecules in the interlayer space, the asymmetric CH_2 stretching vibrations observed at 3030, 2992, 2950, and 2883 cm^{-1} are shifted to 2977, 2934, and 2888 cm^{-1} in the infrared spectrum of the intercalate (Figure 4). The change from 3034, 2954, and 2810 cm^{-1} to 3074, 2937, and 2887 cm^{-1} is observed in the Raman spectrum (Figure 5).

The infrared and Raman spectra of polycrystalline 18-crown-6 and 18-crown-6-intercalated vanadyl phosphate are given in Figures 6 and 7. Like for the dioxane and trioxane intercalates, the intense band at 943 cm^{-1} in

the Raman spectrum of the 18-crown-6 intercalate corresponds to the symmetric $\nu(PO_4)$ vibration. The sharp band at 992 cm^{-1} originates in the V═O stretching vibration. Its position corresponds to the fact that the 18-crown-6 intercalate is thermally very stable as its diffractograms do not change up to 160 °C. The band at about 1035 cm^{-1} in the Raman spectrum may be ascribed to the asymmetric $\nu(PO_4)$ vibration. With the help of the Raman spectrum, we assigned the band at 962 cm^{-1} in the infrared spectrum to the symmetric $\nu(PO_4)$ stretching vibration, which is infrared active because of the distortion of the phosphate tetrahedron in the intercalate. This band is overlapped by a symmetric ring vibration of 18-crown-6, which is observed at 967 cm^{-1} in the spectrum of the pure guest. The small shoulder at 995 cm^{-1} in the infrared spectrum is most probably the V═O stretching band of the vanadyl group. Its position corresponds to the coordination of the guest oxygen atom to vanadium in the intercalate. The asymmetric $\nu(PO_4)$ vibration is overlapped by a strong band of the asymmetric ring vibration of 18-crown-6 observed at 1109 cm^{-1} in the infrared spectrum of the pure guest. Different modes of the CH_2 bending vibrations of polycrystalline 18-crown-6 at 1473, 1351, 1281, and 1249 cm^{-1} are observed at 1461, 1352, 1284, and 1251 cm^{-1} in the infrared spectrum of the intercalate. As in the case of dioxane and trioxane, changes caused by the intercalation are observed in the high-frequency region of the spectrum, where the asymmetric CH_2 stretching vibrations at 2954, 2899, and 2825 cm^{-1} are shifted to 2962, 2917, and 2880 in the infrared spectrum (Figure 6). The changes from 2951, 2897, 2877, 2844, and 2812 cm^{-1} to 2962, 2877, and 2809 cm^{-1} are observed in the Raman spectrum (Figure 7).

Molecular Simulations. The molecular simulation is suitable for intercalation compounds in which the amounts of the guest and host entities in the formula units are in the ratio of small integer numbers. Therefore, we could not use this simulation for $VOPO_4$·0.43(18-crown-6). Nevertheless, from the value of the basal spacing found for this intercalate, we can deduce that the 18-crown-6 molecules are arranged in the interlayer space in a way similar to that proposed for the poly(ethylene glycol) intercalates.[24]

Structure of the Low-Temperature Phase of $VOPO_4$·$C_4H_8O_2$. Structure of the low-temperature phase is illustrated in Figures 8 and 9. The dioxane molecules in chairlike conformation are anchored to vanadium via one of its oxygen atoms to complete the vanadium octahedron instead of water molecules (see Figure 8). The $V-O_{diox}$ distance found by *SUPRAMOL* is 2.506 Å. This distance is close to the $V-O_{guest}$ distances found for $VOPO_4$·$2H_2O$ (2.23 Å),[1] $VOPO_4$·$2D_2O$ (2.50 Å),[2] $VOPO_4$·(diethylene glycol) (2.4 Å),[31] and $VOPO_4$·tetrahydrofuran (2.41 Å).[31] The bilayer arrangement of the dioxane molecules leads to the basal spacing of 11.54 Å. Figure 9 shows the top view of the structure, the arrangement of the guest molecules in the interlayer space, and the way of the layer stacking. Two successive $VOPO_4$ layers in the $VOPO_4$·$C_4H_8O_2$ intercalate are mutually shifted with respect to the original host structure along the *a*(*b*) axis (see Figure 8). The modeled unit cell of the low-temperature phase was found to be triclinic, be space group *P*1, and have unit cell parameters $a = b = 6.21(1)$ Å, $c = 11.58$ Å, $\alpha = \gamma = 90°$ $\beta = 85.54°$, and $Z = 2$ (two formula units per one unit cell). The fractional coordinates in the unit cell for the low-temperature phase are summarized in Table 1. The calculated density is 1.871 g/cm^3. The experimental density was not determined as the sample decomposed during the measurement. The Rp factor characterizing the agreement between the calculated and experimental diffraction patterns[40] is 20%. This relatively high value of the Rp factor is caused by the structural disorder and needs a more detailed explanation. The disorder indicated by the diffraction patterns was confirmed by the modeling. The structure presented in Figures 8 and 9 is an average structure, obtained from a series of calculated models with the same crystal energy and slightly different tilting angle of the dioxane molecule with respect to the host layer. The O−O−V angle (angle between the O−O axis of dioxane molecule and $V-O_{diox}$ line) varied in the range 128−135°. Consequently, there is a variation in the length of the shift vector, characterizing the mutual position of two successive layers. Another type of disorder comes from the fact that the

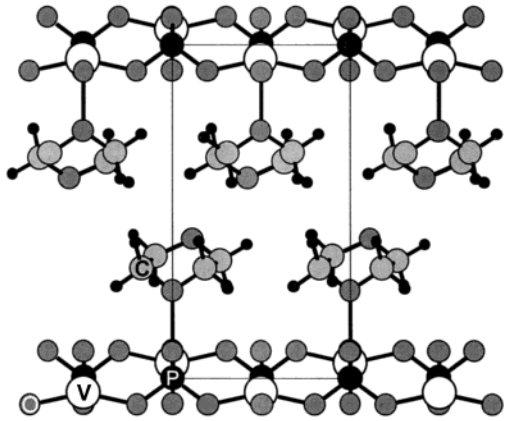

Figure 8. Bilayer arrangement of the dioxane molecules in the interlayer space of vanadyl phosphate in the low-temperature phase of $VOPO_4$·$C_4H_8O_2$, illustrating the anchoring of the guest molecules to the vanadium atoms (open circles, V; light gray circles, C; dark gray circles, O; large black circles, P; small black circles, H atoms).

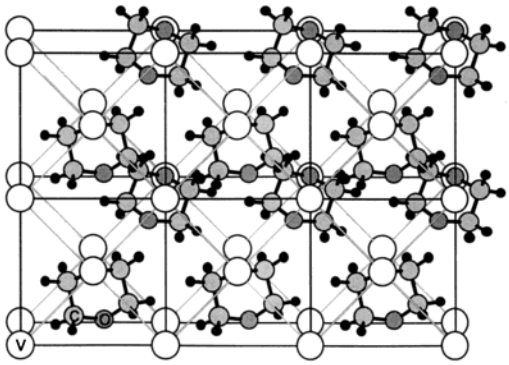

Figure 9. Top view of the $VOPO_4$·$C_4H_8O_2$ structure (l.t.), illustrating the arrangement of the guest molecules and the mutual position of the two successive layers in the intercalated structure. The O and P atoms of the $VOPO_4$ layers are omitted for clarity.

(40) Modern Powder Diffraction. In *Reviews in Mineralogy*; Bish, D. L., Post, J. E., Eds.; Miner. Soc. of America: Washington, DC, 1989; Vol. 20, p 277.

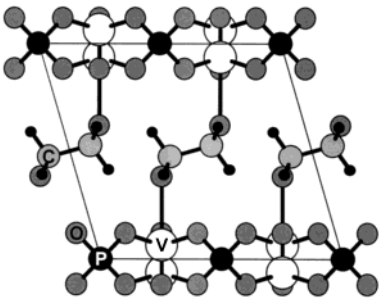

Figure 10. One unit cell of the $VOPO_4 \cdot 0.5C_4H_8O_2$ structure (h.t., space group *C*2/*m*) with the monolayer arrangement of the dioxane molecules anchored to the vanadium atoms with both oxygen atoms.

Table 1. Fractional Coordinates in the Unit Cell with the Space Group *P*1 for the Low-Temperature Phase ($VOPO_4 \cdot C_4H_8O_2$)

atom	*x*	*y*	*z*
O1	0.48648	0.69900	0.07938
O2	−0.01162	0.50000	0.08002
P3	0.00000	0.00000	0.00000
V4	0.00632	0.50000	−0.04353
O5	0.49048	0.30100	0.07938
O6	0.78948	−0.00200	0.07938
P7	0.50000	0.50000	0.00000
O8	0.18748	0.00200	0.07938
O9	0.01352	0.80100	−0.07938
O10	0.51162	0.00000	−0.08002
V11	0.49368	0.00000	0.04353
O12	0.00952	0.19900	−0.07938
O13	0.71052	0.50200	−0.07938
O14	0.31252	0.49800	−0.07938
C15	0.53834	0.82999	0.32644
C16	0.75619	0.90370	0.36287
C17	0.41214	1.18405	0.32670
C18	0.63187	1.26718	0.35000
O19	0.74300	1.11256	0.41443
O20	0.46212	1.00001	0.26063
H21	0.42603	0.78913	0.40306
H22	0.56495	0.68324	0.27224
H23	0.87548	0.90155	0.28587
H24	0.81159	0.78363	0.42580
H25	0.32681	1.30556	0.27652
H26	0.31177	1.15048	0.40902
H27	0.72043	1.30904	0.26593
H28	0.61464	1.41871	0.39713
C29	1.12048	0.67852	0.67563
C30	1.35845	0.63064	0.64690
C31	1.03602	0.31240	0.67292
C32	1.27167	0.25521	0.65757
O33	1.38986	0.42217	0.59637
O34	1.03782	0.50007	0.73932
H35	1.03586	0.70741	0.59568
H36	1.10856	0.82665	0.72963
H37	1.44498	0.64560	0.72723
H38	1.42476	0.75717	0.58559
H39	0.94519	0.18127	0.72043
H40	0.96660	0.33546	0.58764
H41	1.32980	0.22299	0.74425
H42	1.29097	0.10308	0.61115

tetragonal symmetry of the host layer allows an anchoring of the dioxane molecule to the vanadium atom in four equivalent positions symmetrically related thanks to the 4-fold axis in the V−O bond. This type of disorder occurs in $VOPO_4$ intercalation compounds.[31] Consequently, the real structure consists of domains with four types of orientations and the lattice strain in the domain boundaries contributes to the low resolution of the diffraction pattern, especially the broadening of the *hk*0 and *hkl* reflections. The interlayer packing of the guest molecules requires the shift of two successive host

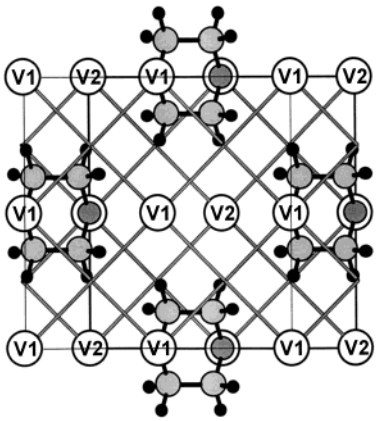

Figure 11. Top view of the $VOPO_4 \cdot 0.5C_4H_8O_2$ structure (h.t.), showing the arrangement of the dioxane molecules in the interlayer space and the mutual positions of the two successive layers (V1, vanadium atoms of the upper layer; V2, vanadium atoms of the lower layer). The O and P atoms of the $VOPO_4$ layers are omitted for clarity.

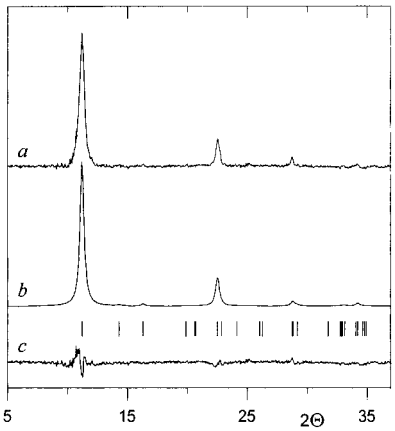

Figure 12. Comparison of the experimental (a) and calculated (b) diffraction patterns and the difference curve (c) for the high-temperature phase ($VOPO_4 \cdot 0.5C_4H_8O_2$). The Rp factor is 6.7%.

Table 2. Fractional Coordinates in the Unit Cell with the Space Group *C*2/*m* for the High-Temperature Phase ($VOPO_4 \cdot 0.5C_4H_8O_2$)

atom	*x*	*y*	*z*
P1	0.50000	−0.25043	0.00000
O1	0.28081	−0.50000	0.11931
V1	0.23324	−0.50000	−0.06491
O2	0.63106	−0.34893	0.11835
O3	0.43006	−0.15193	0.11835
C1	−0.09268	−0.63440	−0.52755
O4	0.15160	−0.50000	−0.38113
H1	−0.13668	−0.64433	−0.41235
H2	−0.14079	−0.73288	−0.61105

layers, resulting in the lowering of the tetragonal symmetry to the triclinic one (space group *P*1).

Structure of the High-Temperature Phase of $VOPO_4 \cdot 0.5C_4H_8O_2$. Each molecule of dioxane in the chairlike conformation is anchored to vanadium in lower and upper layers with both of its oxygen atoms. It means that the layers are linked via dioxane molecules (Figure 10). The $V-O_{diox}$ distance found by *SUPRAMOL* is 2.495 Å. Figure 10 shows one unit cell in side view, illustrating the monolayer arrangement of the guest molecules. In this case the basal spacing is 7.89 Å. Figure 11 shows the top view of the structure, the arrangement of the guest molecules in the interlayer space, and the way of

the layer stacking. Two successive $VOPO_4$ layers in the $VOPO_4 \cdot 0.5C_4H_8O_2$ intercalate are shifted toward each other with respect to the original host structure along the *ab* diagonal. The modeled unit cell of the high-temperature phase is monoclinic, is space group *C*2/*m*, and has unit cell parameters $a = b = 8.94$ Å, $c = 8.22$ Å, $\alpha = \gamma = 90°$, $\beta = 106.30°$, and $Z = 4$. The calculated density of 2.248 g/cm^3 is in a good agreement with the experimental value of 2.26 g/cm^3. The fractional coordinates in the unit cell for the high-temperature phase are summarized in Table 2. The Rp factor in this case is 6.7% after the correction of the diffraction data for the preferred orientation according to March-Dollase[41] and the comparison of calculated and experimental diffraction patterns is given in Figure 12. The attachment of each guest molecule to the lower and upper host layers leads to a regular layer stacking without disorder. This effect is accompanied by a significant lowering of the Rp factor in comparison with the low-temperature phase.

Acknowledgment. The Grant Agency of the Czech Republic (Grant 202/01/0520) supported this work. The help of the Ministry of Education, Youth and Sports of the Czech Republic (MSM113200001 and MSM253100001) and the Academy of Sciences of the Czech Republic (AV0Z4050913) is appreciated.

CM021134+

(41) Dollase, W. A. *J. Appl. Crystallogr.* **1986**, *19*, 267−272.